Incoherent optical conductivity and breakdown of the generalized Drude formula in quasi-one-dimensional bad metallic systems

Kupčić, Ivan

Incoherent optical conductivity and breakdown of the generalized Drude formula in quasi-one-dimensional bad metallic systems

I. Kupčić
Department of Physics, Faculty of Science, University of Zagreb, P.O. Box 331, HR-10002 Zagreb, Croatia
(Received 27 February 2009; published 2 June 2009)

The high-energy (HE) intraband optical processes in a wide class of strongly correlated quasi-one-dimensional systems are explained in a way that is consistent with the Fermi golden rule, by using the force-force correlation function (FFCF) theory. It turns out that these processes must be distinguished from the related low-energy (LE) optical processes of the generalized Drude formula by making use of two different summations of Feynman diagrams, which include, respectively, the large-momentum and $\mathbf{q}\approx 0$ electron-hole excitations. Using the FFCF approach, the common expression for the single-particle optical conductivity of clean charge-density-wave (CDW) systems is rederived and the formation of the CDW gap in the optical conductivity of dirty CDW systems is briefly discussed. It is argued that the clear distinction between the HE and LE intraband optical processes is required whenever the electrical/optical conductivity of conduction electrons is predominantly incoherent, including the cases of bad metallic compounds and various heavy-electron systems.

DOI: 10.1103/PhysRevB.79.235104 PACS number(s): 71.45.Lr, 78.20.Bh, 71.30.+h, 71.28.+d

I. INTRODUCTION

During the last three decades, a rich variety of metallic compounds has been investigated whose room temperature $\omega\approx 0$ conductivity is found to be on the order of 2000 $(\Omega\ \mathrm{cm})^{-1}$, the value smaller for a factor of 25 than that characterizing conventional metals of nearly the same concentration of conduction electrons. Among the most intriguing examples are the high-T_c superconductors,[1] various quasi-one-dimensional (Q1D) systems with the charge-density-wave (CDW) or the spin-density-wave instability,[2,3] as well as various heavy-electron systems.[4,5] The common Kramers-Kronig analyses of the measured reflectivity data usually reveal an effective intraband energy scale on the order of 0.5–1 eV. This scale is identified as representing the high-energy (HE) intraband relaxation rate and is associated with the regime of large effective electron mass in the generalized Drude formula. However, it proves that theoretical models based on the description of single-particle intraband optical excitations in terms of $\mathbf{q}\approx 0$ intraband electron-hole pairs,[6–8] including the phenomenological generalized Drude formula, are not suitable for explaining the HE part of measured spectra. Therefore, the generalized Drude formula breaks down whenever the uncertainty in the energy of HE electron-hole excitations becomes larger than a fraction of the bandwidth. We shall show here that the solution of this problem lies in treating the HE intraband optical processes in a way consistent with the HE Fermi golden rule.

The appearance of a large effective intraband energy scale in the optical conductivity of heavy-electron compounds is recently recognized[9] as a clear evidence for the two-component intraband electrical/optical conductivity. On qualitative grounds, it is argued that the first component reflects the coherent low-energy (LE) electrical conductivity. It is described by the Drude formula, but with a presumably small intraband relaxation rate and a small effective number of conduction electrons. The second, nearly featureless, component is ascribed to the incoherent conductivity processes, which are present at energies up to W (W is the width of the conduction band and represents the maximal value for the energy of real large-momentum intraband electron-hole excitations). The large effective energy scale mentioned above is explained in simple physical terms as the effective bandwidth.[9]

The prototype bad metallic system $BaVS_3$ is in many aspects similar to simple heavy-electron systems. $BaVS_3$ possesses the Q1D crystal structure,[10] and is characterized, in addition to the structural phase transition at $T_S\approx 240$ K (Ref. 11) and the magnetic transition at $T_\chi\approx 40$ K,[12] by the CDW metal-to-insulator phase transition at $T_{MI}\approx 70$ K.[11,13] Particularly important are the recent optical conductivity results[14] which shed a new light on anomalies observed earlier by other experimental methods.[11,13,15,16] It is shown that the optical conductivity in the direction perpendicular to the highly conducting chain axis **c** is almost completely incoherent. In the highly conducting direction, on the other hand, it is found that only 15% of the total spectral weight corresponds to the Drude-type intersite processes (the effective electron mass parameter m_{eff}, to be defined later, is estimated to be $m_{\mathrm{eff}}\approx 7m$), while the rest of the spectral weight is shared between the incoherent frequency-independent intersite contributions and the HE onsite contributions. The dc conductivity at $T>T_{MI}$, together with the related dc limit of the optical conductivity, is found to be almost isotropic $(\sigma_{\parallel}^{\mathrm{dc}}/\sigma_{\perp}^{\mathrm{dc}}\approx 3-4)$. In this paper, we will argue that such surprisingly small anisotropy of the dc conductivity is closely related with the incoherent nature of electrical conductivity. Moreover, we will show that a rather unusual profile of the CDW gap in the optical conductivity (clearly seen for both polarizations of the external electromagnetic fields) with a maximum well above the CDW threshold energy 2Δ (with Δ estimated from the activation behavior of the transport coefficients) could also be considered as a clear manifestation of the conductivity which is predominantly incoherent.

From the theoretical standpoint, one of the central questions regarding the incoherent conductivity in $BaVS_3$, as well

as in similar bad metallic systems, is to derive the microscopic model for the two-component intraband optical conductivity. In other words, it is necessary to formulate the response theory which will be able to explain both the LE electrical conductivity, closely related to the various dc transport coefficients, and the HE intraband optical excitations. In this spirit, in Secs. III and IV we will address the issue of the longitudinal LE and the transverse HE response theories, by considering a simple Q1D model for conduction electrons, and discuss the adventages and disadvantages of the two approaches. The examination of the HE optical conductivity of clean and dirty CDW systems, with still simple bare electron dispersions, is postponed to Sec. V. A more detailed microscopic description of conduction electrons, together with the answers to several specific questions concerning $BaVS_3$, will be given in a separate paper.[17] Before turning to the detailed discussion of the questions which were just mentioned, let us recall the basic qualitative ideas concerning the incoherent conductivity in heavy-electron systems.

II. INCOHERENT ELECTRICAL CONDUCTIVITY

From the work of Gunnarsson *et al.*,[9] it is known that an appropriate starting point for qualitative analysis of the electrical and optical conductivity in heavy-electron systems is to consider the total conductivity spectral weight measured for all relevant polarizations of the external electromagnetic fields. In their work, the emphasis was on the understanding of the distribution of the total spectral weight over the LE and HE regions, up to energies on the order of the natural intraband cutoff energy, the bandwidth W.

The present discussion of the bad metallic conductivity regime relies on the observation that the experimentally determined optical conductivity in bad metals[14] is very much reminiscent of that of heavy-electron systems.[5] The difference is that in bad metallic systems the effective electron mass $m_{\rm eff}$ is typically below $10m$, while in heavy-electron systems it amounts to several tens of m. Evidently, none of these two regimes can be fully reconciled with the electrical conductivity model based exclusively on the electron-phonon and electron-static-disorder scattering mechanisms. Thus, the strong local interactions must be considered to explain quantitatively the electrodynamic properties of such systems. The strong local interactions manifest themselves, in the first place, in a large renormalization of the effective electron mass, compared with the bare electron mass m. The transfer of a large portion of the LE spectral weight into the HE region takes place in addition as a function of temperature. However, to make the presentation of the results in Secs. III–V as simple as possible, the strong electron scattering will be interpreted as arising from the strong scattering on the static disorder, even though, strictly speaking, this type of electron scattering processes does not renormalize $m_{\rm eff}$ very much. In what follows, in particular in Sec. IV, the generalization to the proper physical situation with strong local interactions is straightforward, but the quantitative results are very sensitive to the details in the interaction Hamiltonian.

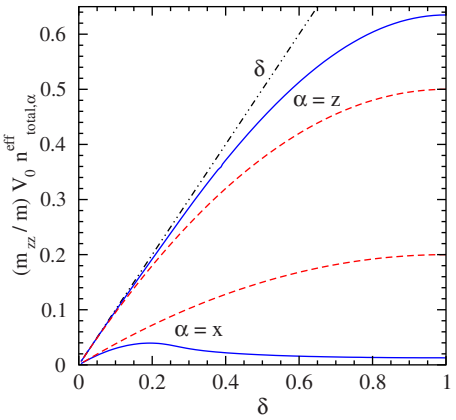

FIG. 1. (Color online) The solid lines represent the effective numbers $\tilde{n}^{\rm eff}_{{\rm total},\alpha}=(m_{zz}/m)V_0 n^{\rm eff}_{{\rm total},\alpha}$, $\alpha=z,x$, as a function of the electron doping δ in the coherent conductivity regime, for the Q1D single-band model $\varepsilon(\mathbf{k})=-2t_{\parallel}\cos\mathbf{k}\cdot\mathbf{c}-2t_{\perp}\cos\mathbf{k}\cdot\mathbf{a}$, with $2t_{\parallel}=1$ eV, $2t_{\perp}=0.1$ eV, $a/c=2$, and $T=100$ K. The dashed lines show the results of the completely incoherent conductivity regime.

A. Total spectral weight

For further considerations it is appropriate to recall the tight-binding expression for the total conductivity spectral weight,

$$\frac{1}{2}\Omega^2_{{\rm total},\alpha}=\frac{2\pi e^2}{m}n^{\rm eff}_{{\rm total},\alpha}\equiv\frac{1}{2}\Omega_0^2\frac{m}{m_{zz}}\tilde{n}^{\rm eff}_{{\rm total},\alpha}. \tag{1}$$

In this expression $\tilde{n}^{\rm eff}_{{\rm total},\alpha}$ is the total effective number of charge carriers in the conduction band normalized in the way that $\tilde{n}^{\rm eff}_{{\rm total},\parallel}\approx\delta$ for $\delta\to 0$ (see Fig. 1); δ is the number of conduction electrons per primitive cell. When shown in the representation of the localized atomic orbitals, it takes the form

$$\tilde{n}^{\rm eff}_{{\rm total},\alpha}=\frac{1}{2N}\sum_{i\delta\sigma}\frac{r^2_{\delta\alpha}}{c^2}\frac{t_\delta}{t_{\parallel}}\langle c^{\dagger}_{i+\delta\sigma}c_{i\sigma}\rangle. \tag{2}$$

The vector $\mathbf{r}_\delta$ runs over the first neighbors of the considered site $\mathbf{r}_i$, and t_δ is the related hopping integral (the bond energy, in common language). $\Omega_0=\sqrt{4\pi e^2/(mV_0)}$ is an auxiliary frequency scale, V_0 is the primitive cell volume, and $m_{zz}=\hbar^2/(2t_{\parallel}c^2)$ is the mass scale parameter. Of course, $2t_{\parallel}\tilde{n}^{\rm eff}_{{\rm total},\alpha}$ can also be interpreted as representing the average kinetic (hopping) energy, whereas $\langle c^{\dagger}_{i+\delta\sigma}c_{i\sigma}\rangle$ is the average bond representing the probability for an electron to hop from the site $\mathbf{r}_i$ to the site $\mathbf{r}_i+\mathbf{r}_\delta$. In the completely coherent regime, this probability has the well-known form,[18] while in the completely incoherent regime it is given simply by $\tilde{n}^{\rm eff}_{{\rm total},\parallel}\approx\delta(1-\delta/2)$ (Ref. 9) and $\tilde{n}^{\rm eff}_{{\rm total},\perp}\approx(a/c)^2(t_\perp/t_{\parallel})\tilde{n}^{\rm eff}_{{\rm total},\parallel}$.

The results are illustrated in Fig. 1 for the usual Q1D single-band model $\varepsilon(\mathbf{k})=-2t_{\parallel}\cos\mathbf{k}\cdot\mathbf{c}-2t_{\perp}\cos\mathbf{k}\cdot\mathbf{a}$, for both conductivity regimes. A substantial difference between the two conductivity regimes occurs only for the open Fermi surfaces ($0.2\lesssim\delta\lesssim 1.8$ for the parameters used in the figure), where an extra factor $(t_\perp/t_{\parallel})$ arises in $\tilde{n}^{\rm eff}_{{\rm total},\perp}$ in the coherent conductivity regime. The anisotropy of the dc conductivity in the strongly correlated Q1D systems (related to $\tilde{n}^{\rm eff}_{{\rm total},\alpha}$ in the

way shown below) is expected to be profoundly influenced by the incoherent nature of the electrical conductivity. The incoherent conductivity is thus the subject of easy observation in the Q1D systems, not only through the anomalous shape of the HE optical conductivity, but also through almost isotropic $\omega \approx 0$ properties.

B. Empirical electrical conductivity formula

In the vast majority of heavy-electron systems at least two contributions can be distinctly resolved in the measured optical conductivity spectra. They are usually fitted to a simple two-component formula[6,9]

$$\mathrm{Re}\{\sigma_{\alpha\alpha}(\omega)\} = \delta\frac{\hbar\Omega_0^2}{4\pi}\left[\frac{(n_{\alpha\alpha}^{\mathrm{eff}}/n)\Gamma_\alpha}{\hbar(\omega^2+\Gamma_\alpha^2)} + \frac{\pi(n_{\mathrm{incoh},\alpha}^{\mathrm{eff}}/n)}{2\tilde{W}}\right]. \quad (3)$$

Here, $n_{\alpha\alpha}^{\mathrm{eff}}$ is the effective number of conduction electrons, $n_{\mathrm{incoh},\alpha}^{\mathrm{eff}} = n_{\mathrm{total},\alpha}^{\mathrm{eff}} - n_{\alpha\alpha}^{\mathrm{eff}}$, Γ_α is the transport relaxation rate, and $\tilde{W}$ is the effective bandwidth. Finally, $\hbar\Omega_0^2/(4\pi\ \mathrm{eV})$ is a useful conductivity scale.

The good and the bad metallic conductivity regimes in Eq. (3) are associated with $n_{\mathrm{incoh},\alpha}^{\mathrm{eff}} \approx 0$ and $n_{\alpha\alpha}^{\mathrm{eff}} \ll n$, respectively. In the former case, $\sigma_{\alpha\alpha}^{\mathrm{dc}} = \mathrm{Re}\{\sigma_{\alpha\alpha}(0)\} \gg \delta\hbar\Omega_0^2/(4\pi\ \mathrm{eV})$, giving rise to $n_{\alpha\alpha}^{\mathrm{eff}}/n \gg \hbar\Gamma_\alpha/\mathrm{eV}$ and $\hbar\Gamma_\alpha$ on the order of 50 meV. In the latter case, $(n_{\alpha\alpha}^{\mathrm{eff}}/n)/(\hbar\Gamma_\alpha) + \pi(n_{\mathrm{incoh},\alpha}^{\mathrm{eff}}/n)/(2\tilde{W}) \approx 1/\mathrm{eV}$, resulting typically in $\tilde{W} \approx 0.5-1$ eV, and in the Ioffe-Regel conductivity at large enough temperatures (where $n_{\alpha\alpha}^{\mathrm{eff}} = 0$).[9] Actually, in the latter case, the parameters $n_{\alpha\alpha}^{\mathrm{eff}}$ and Γ_α are both frequency dependent [i.e., the first term in the brackets in Eq. (3) is the generalized Drude term]. Although the theoretical models widely used to study heavy-electron systems account well for the LE part of the spectra at low enough temperatures (in particular the observed dependence of $n_{\alpha\alpha}^{\mathrm{eff}}$ and Γ_α on frequency), they usually fail to reproduce the HE part of the spectra (for a detailed discussion of this topic the reader is referred to Ref. 5).

III. LOW-ENERGY INTRABAND EXCITATIONS

The conduction electrons generally scatter on the static disorder [described by the single-particle interaction $V_1(\mathbf{q}')$ independent of time] or interact through the various nonretarded two-particle short-range interactions or through the retarded boson-mediated interactions. All these scattering mechanisms are described here in terms of the *intraband* electron-boson coupling $G_\lambda(\mathbf{q}')$, the boson propagator $\mathcal{D}_\lambda(\mathbf{q}',\tau)$, and the boson frequency $\omega_{\lambda\mathbf{q}'}$ (λ is the boson branch index, with the scattering on the static disorder labeled by $\lambda=0$). In Sec. IV, the product of $\mathcal{D}_\lambda(\mathbf{q}',\tau)$ and $|G_\lambda(\mathbf{q}')|^2/N$ is called the force-force correlation function,[19] and is denoted by $\mathcal{F}_\lambda(\mathbf{q}',\tau) = (|G_\lambda(\mathbf{q}')|^2/N)\mathcal{D}_\lambda(\mathbf{q}',\tau) \equiv -\langle T_\tau[\Psi_\lambda(\mathbf{q}',\tau)\Psi_\lambda(-\mathbf{q}',0)\rangle$. The generalization to the case in which the *interband* electron-scattering processes are treated explicitly is straightforward, but these processes are not of qualitative importance in discussing the main points of this paper.

The key parameter of the present analysis is the ratio between the largest coupling constant $G_\lambda(\mathbf{q}')$ and the bandwidth W. The bad metallic conductivity regime of Eq. (3) is expected in the cases where $G_\lambda(\mathbf{q}')/W$ becomes comparable to unity or larger. As mentioned above, the regime of strong interactions $V_1(\mathbf{q}')$ is used throughout this paper, but only for illustration purposes. In this case, $\mathcal{D}_0(\mathbf{q}',\tau)$ is independent of time and $\sqrt{N}V_1(\mathbf{q}')/W \approx 1$.

A. Longitudinal response theory

In the longitudinal field-theory approach, the LE intraband single-particle excitations are naturally described by the Bethe-Salpeter equations for $\mathbf{q} \approx 0$ electron-hole pairs, combined with the Dyson equations for single-electron propagators.[20] The fundamental questions of the Ward identity and the related charge continuity equation can be answered by using the modified Dyson equations for electrons from the outset. In this case only those scattering processes are taken into account that survive the cancellations by the vertex corrections in the Bethe-Salpeter equations.[21] Formally, the other (forward) scattering processes are eliminated by replacing the coupling constants $|G_\lambda(\mathbf{q}')|^2$ in the single-electron self-energy by $|G_\lambda(\mathbf{q}')|^2[1-J_\alpha(\mathbf{k}+\mathbf{q}')/J_\alpha(\mathbf{k})]$. The Bloch energy $\varepsilon(\mathbf{k})$ corresponds to the position of the quasiparticle pole in the modified single-electron Green's function and is the sum of its bare value, $\varepsilon^0(\mathbf{k})$, and the self-energy corrections. The intraband current vertices $J_\alpha(\mathbf{k})$ are also affected by these corrections through the common relation $J_\alpha(\mathbf{k}) = ev_\alpha(\mathbf{k}) = (e/\hbar)\partial\varepsilon(\mathbf{k})/\partial k_\alpha$ [$v_\alpha(\mathbf{k})$ is the electron group velocity]. In most cases of interest, the $\mathbf{q} \approx 0$ electron-hole propagator is a simple product of two modified single-electron Green's functions, in full analogy with the perfect metallic case. The final result, expressed in terms of the induced charge and current densities, is identical to the common transport equations.[19,22,23] This seems to be the appropriate procedure, at least, for the parameters $G_\lambda(\mathbf{q}')/W$ which are sufficiently small.

The electrical conductivity is given by the generalized Drude formula

$$\sigma_{\alpha\alpha}(\omega) = \frac{1}{V}\sum_{\mathbf{k}\sigma} J_\alpha^2(\mathbf{k})(-)\frac{\partial f(\mathbf{k})}{\partial\varepsilon(\mathbf{k})}\frac{i}{\omega+\Pi_\alpha(\mathbf{k},\omega)}. \quad (4)$$

Here $\Pi_\alpha(\mathbf{k},\omega)$ is the electron-hole-pair self-energy, which is the result of the analytical continuation $(i\nu_n \to \omega + i\eta)$ of

$$\Pi_\alpha(\mathbf{k},\mathbf{k}_+,i\nu_n) = \tilde{\Sigma}[\mathbf{k},\varepsilon(\mathbf{k}_+)/\hbar - i\nu_n] - \tilde{\Sigma}[\mathbf{k}_+,\varepsilon(\mathbf{k})/\hbar + i\nu_n]. \quad (5)$$

$\tilde{\Sigma}(\mathbf{k},i\omega_n)$ is the single-electron self-energy in the modified Dyson equation,

$$\hbar\tilde{\Sigma}(\mathbf{k},i\omega_n) \approx \sum_{\lambda\mathbf{q}'}\sum_{s=+1,-1}\frac{|G_\lambda(\mathbf{q}')|^2}{N} \times\left[1-\frac{J_\alpha(\mathbf{k}+\mathbf{q}')}{J_\alpha(\mathbf{k})}\right]\frac{f_\lambda^b(\mathbf{q}')+f[s\varepsilon(\mathbf{k}+\mathbf{q}')]}{i\hbar\omega_n-\varepsilon(\mathbf{k}+\mathbf{q}')+s\hbar\omega_{\lambda\mathbf{q}'}} \quad (6)$$

(the index λ runs over all scattering channels and $\mathbf{k}_+ = \mathbf{k}+\mathbf{q}$).

In a large majority of good metals the expression in Eq. (4) can be further simplified to give

$$\sigma_{\alpha\alpha}(\omega) \approx \frac{e^2 n^{\rm eff}_{{\rm intra},\alpha}}{m} \frac{i}{\omega + \Pi_\alpha(\mathbf{k}_F,\omega)}. \tag{7}$$

In this expression,

$$n^{\rm eff}_{{\rm intra},\alpha} = \frac{m}{e^2}\frac{1}{V}\sum_{\mathbf{k}\sigma} J^2_\alpha(\mathbf{k})(-)\frac{\partial f(\mathbf{k})}{\partial \varepsilon(\mathbf{k})} \tag{8}$$

represents the bare effective number of conduction electrons. It is important to realize here that the derivative $\partial f(\mathbf{k})/\partial\varepsilon(\mathbf{k})$ in Eq. (4) is a consequence of the fact that the electron-hole pairs used to formulate elementary single-particle excitations are ascribed to the single-particle states in the thermal window around the Fermi energy, irrespective of the frequency of external fields. This represents the principal weakness in explaining the HE optical processes of the generalized Drude formula [Eq. (4)], or of any similar longitudinal field-theory expression (Refs. 7 and 8).

B. Effective electron mass parameter

The relaxation processes in the common good metals are largely due to the electron scattering on phonons. Since the related parameter $G_\lambda(\mathbf{q}')/W$ is small, Eq. (5) reduces to the ordinary Drude formula with $\Pi_\alpha(\mathbf{k}_F,\omega)\approx\omega\lambda_\alpha+(1+\lambda_\alpha)i\Gamma_\alpha$, and $\mathrm{Re}\{\sigma^{\rm HE}_{\alpha\alpha}(\omega)\}\approx\sigma_{\alpha\alpha}(0)(\Gamma_\alpha/\omega)^2$ in the HE region. The effective number of conduction electrons $n^{\rm eff}_{\alpha\alpha}$, introduced phenomenologically by Eq. (3), is given now by $n^{\rm eff}_{\alpha\alpha}=n^{\rm eff}_{{\rm intra},\alpha}/(1+\lambda_\alpha)\equiv(m/m_{\rm eff})n$.

It is well known that the scattering on the static disorder [incorporated in the present theory through the replacement $\omega_{0\mathbf{q}'}\to 0$ and $[1+2f^b_0(\mathbf{q}')]|G_0(\mathbf{q}')|^2\to N|V_1(\mathbf{q}')|^2$ in Eq. (6)] does not renormalize $m_{\rm eff}$ very much, whereas the electron scattering on phonons results typically in $m_{\rm eff}$ between m and $2m$.[19]

C. HE excitations

Explaining the HE intraband excitations in the bad metallic systems or in other strongly correlated electronic systems, where $\mathrm{Re}\{\sigma^{\rm HE}_{\alpha\alpha}(\omega)\}\propto\omega^{-\nu}$ is observed in experiments with the exponent ν well below 2, is a challenge for the common field-theory approaches. The proper theory must include both the strong electron correlations and more importantly, the various electron scattering processes not included in the ordinary Drude formula, but allowed by the HE Fermi golden rule. The point is that the essential diagrams encountered in the HE intraband processes differ from those used to describe the dc transport properties. As demonstrated in Sec. IV, in order to catch the essential processes of this kind, one must collect the diagrams in powers of $|G_\lambda(\mathbf{q}')|^2$ to infinity by using the large-momentum Bethe-Salpeter equations, instead of the $\mathbf{q}\approx 0$ Bethe-Salpeter equations of Sec. III A.[21]

For the purpose of comparison with Sec. IV B, as well as to clarify the last statements, we allow the energy scale $\sqrt{N}V_1(\mathbf{q}')$ to be as large as the bandwidth W and take the other electron scattering channels aside. The HE optical excitations in $\Delta\sigma^{\rm HE}_{\alpha\alpha}(\omega)=\sigma^{\rm HE}_{\alpha\alpha}(\omega)-ie^2n^{\rm eff}_{{\rm intra},\alpha}/(m\omega)$ are present now up to the cutoff energy $\varepsilon_{\max}(\mathbf{k}',\mathbf{k}_F)$ and characterized by a complicated frequency dependence which is very different from the Drude $\nu=2$ law. This is evident from the expansion of Eq. (4) in powers of $|V_1(\mathbf{q}')|^2$ to the linear term ($\mathbf{q}'=\mathbf{k}'-\mathbf{k}$),

$$\Delta\sigma^{\rm HE}_{\alpha\alpha}(\omega) \approx \frac{i\hbar}{V}\sum_{\mathbf{k}\sigma} J^2_\alpha(\mathbf{k})\frac{\partial f(\mathbf{k})}{\partial\varepsilon(\mathbf{k})}\sum_{\mathbf{k}'}\frac{|V_1(\mathbf{k}'-\mathbf{k})|^2}{\varepsilon^2(\mathbf{k},\mathbf{k}')}\left\{1-\frac{J_\alpha(\mathbf{k}')}{J_\alpha(\mathbf{k})}\right\} \times\left[\frac{1}{\hbar\omega+i\eta+\varepsilon(\mathbf{k},\mathbf{k}')}+\frac{1}{\hbar\omega+i\eta+\varepsilon(\mathbf{k}',\mathbf{k})}\right] \tag{9}$$

[$\varepsilon(\mathbf{k}',\mathbf{k})=\varepsilon(\mathbf{k}')-\varepsilon(\mathbf{k})$ is a useful abbreviation].

The generalized Drude formula [Eq. (4)], the elastic electron scattering result in Eq. (9) as well as the extension of Eq. (9) to a very general case with boson-mediated interactions are all incomplete in the regime of strong electron scattering. As pointed out above, this is principally due to the fact that all single-particle excitations in such conductivity models are described in terms of the electron-hole pairs of the wave vectors $\mathbf{k}$ and $\mathbf{k}+\mathbf{q}$. The damping energies $\hbar\Gamma_\alpha(\omega)=\mathrm{Im}\{\hbar\Pi_\alpha(\mathbf{k}_F,\omega)\}$ larger than 0.5 eV are required to explain the measured intraband optical conductivity at energies on the order of 0.5 eV, or larger, as demonstrated, for example, in Refs. 1 and 7. Such explanations of the HE optical excitations turn out to be accompanied by the apparent violation of the energy conservation law. They are also too crude to predict correctly the proper cutoff energy for the intraband relaxation processes [$\varepsilon_{\max}(\mathbf{k}',\mathbf{k})=W$, as pointed out in Sec. I]. Our purpose to overcome these two problems and to make a meaningful comparison with the experimental data compels us to go beyond the generalized Drude formula [Eq. (4)].

IV. HIGH-ENERGY INTRABAND EXCITATIONS

The analysis presented in this section is the extension of the equation-of-motion approach of Refs. 24 and 25 to a very general case with the time-dependent FFCF.[19] In Ref. 24, it is shown that in the clean Q1D metallic/semiconducting systems it is possible to formulate the unified gauge-invariant response theory for the longitudinal and transverse correlation functions only if a clear distinction is drawn between the so-called direct ($\mathbf{q}\approx 0$) and indirect (large-momentum) electron scattering processes. It is demonstrated in addition in Ref. 25 that the same distinction is required to make a consistent field-theory description of the long-range screening in electronic Raman scattering experiments in the high-T_c superconductors.

In this section, we shall first derive the FFCF formulae for the optical conductivity. The results will then be applied to the usual metallic case in Sec. IV B. The optical excitations in the ordered clean and dirty CDW systems will be briefly discussed in Sec. V.

A. Force-force correlation function approach

The FFCF approach represents the natural way to reveal the connection between the HE intraband optical processes

and the real electron-hole excitations.[19] Although it is usually focused on the HE intraband optical excitations in a single band, the generalization to more complicated optical processes is straightforward. Thus, this approach would be suitable for investigating the HE intraband excitations in a variety of strongly correlated systems.

In this subsection, we consider the single-band case. The coherent electron scattering on the CDW potential is the simplest (exactly solvable) example in which both the intraband and interband optical excitations are present. We show in Sec. V A that the FFCF theory presented in this subsection accounts well for the clean CDW case as well, provided the single-band representation for conduction electrons is replaced by the related two-band representation.

The convenient starting point for the FFCF analysis is the current-current correlation function[19,26]

$$\Pi_{\alpha\alpha}(\omega) = \frac{1}{(\hbar\omega)^2}[\phi_{\alpha\alpha}(\omega) - \phi_{\alpha\alpha}(0)]. \tag{10}$$

Here $\phi_{\alpha\alpha}(\omega)$ is obtained by the analytical continuation of the auxiliary current-current correlation function $\phi_{\alpha\alpha}(i\nu_n)$ defined by

$$\frac{\phi_{\alpha\alpha}(i\nu_n)}{(i\hbar\nu_n)^2} = \frac{1}{\beta V}\sum_{i\omega_n\mathbf{k}\mathbf{k}'\sigma} J_\alpha(\mathbf{k})J_\alpha(\mathbf{k}')\Phi(\mathbf{k},\mathbf{k}_+,\mathbf{k}'_+,\mathbf{k}',i\omega_n,i\omega_{n+}). \tag{11}$$

By definition $\Phi(\mathbf{k},\mathbf{k}_+,\mathbf{k}'_+,\mathbf{k}',i\omega_n,i\omega_{n+})$ is the intraband $\mathbf{q}\approx 0$ electron-hole propagator and $i\omega_{n+}=i\omega_n+i\nu_n$. Unlike the case of the longitudinal response theory of Sec. III, here this electron-hole propagator includes only those electron scattering processes whose momentum and energy relaxations on the disorder and the boson modes are accompanied by the creation of real large-momentum electron-hole pairs, as required by the HE Fermi golden rule. Therefore, at high-enough energies, the $\mathbf{q}\approx 0$ electron-hole pairs appear only as the virtual intermediate states between the absorption/emission of a photon and the creation/destruction of the real large-momentum electron-hole pair [see Fig. 2(b)], and in the present theory are joint together with the bare current vertices to give the effective current vertices.

According to Fig. 2(a), the electron-hole propagator in question can be written in the following way

$$\begin{aligned} &J_\alpha(\mathbf{k})J_\alpha(\mathbf{k}')\Phi(\mathbf{k},\mathbf{k}_+,\mathbf{k}'_+,\mathbf{k}',i\omega_n,i\omega_{n+}) \\ &= (-)\frac{1}{\beta\hbar}\sum_{\lambda\mathbf{q}'i\nu_m} j_\alpha(\mathbf{k},\mathbf{k}_+ + \mathbf{q}',i\hbar\omega_{n+},i\hbar\omega_{m-}) \\ &\quad\times\mathcal{F}_\lambda(\mathbf{q}',i\nu_m)\Phi(\mathbf{k},\mathbf{k}_+ + \mathbf{q}',\mathbf{k}'_+ + \mathbf{q}',\mathbf{k}',i\omega_n,i\omega_m) \\ &\quad\times j_\alpha(\mathbf{k}',\mathbf{k}'_+ + \mathbf{q}',i\hbar\omega_{n+},i\hbar\omega_{m-}), \end{aligned} \tag{12}$$

with $\mathcal{F}_\lambda(\mathbf{q}',i\nu_m)=(|G_\lambda(\mathbf{q}')|^2/N)\mathcal{D}_\lambda(\mathbf{q}',i\nu_m)$ and $\mathbf{k}_+\approx\mathbf{k}$ ($i\omega_m=i\omega_n+i\nu_n+i\nu_m$ and $i\omega_{m-}=i\omega_m-i\nu_n$). Both the two regular and the two anomalous contributions to $\phi_{\alpha\alpha}(i\nu_n)$ of Fig. 2(b) are shown here as a function of the large-momentum electron-hole propagator $\Phi(\mathbf{k},\mathbf{k}+\mathbf{q}',\mathbf{k}'+\mathbf{q}',\mathbf{k}',i\omega_n,i\omega_m)$. The latter is determined self-consistently using the large-momentum Bethe-Salpeter equations of Fig. 2(c). Finally,

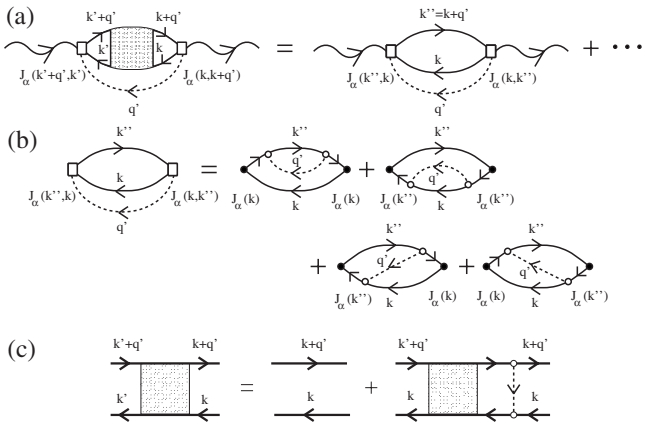

FIG. 2. (a) The auxiliary intraband current-current correlation function in the FFCF approach. (b) The leading term in the HE limit, which consists of two regular and two anomalous contributions. The full circle is the bare current vertex and the open square is the effective current vertex. The dashed line represents the related FFCF. (c) The Bethe-Salpeter equations stands for the large-momentum electron-hole propagators.

$$j_\alpha(\mathbf{k},\mathbf{k}'',i\hbar\omega_{n+},i\hbar\omega_{m-}) = \frac{1}{\hbar}[J_\alpha(\mathbf{k})\mathcal{G}^0(\mathbf{k}_+,i\omega_{n+}) + J_\alpha(\mathbf{k}'')\mathcal{G}^0(\mathbf{k}''_-,i\omega_{m-})] \tag{13}$$

is the effective current vertex, and $\mathcal{G}^0(\mathbf{k},i\omega_n)$ is the bare single-electron Green's function. The optical conductivity is given by the Kubo formula for optical conductivity

$$\sigma_{\alpha\alpha}(\omega) = \frac{i}{\omega}[\Pi_{\alpha\alpha}(\omega) - \mathrm{Re}\{\Pi_{\alpha\alpha}(0)\}]. \tag{14}$$

The second term in the brackets takes care of the cancellation of the diamagnetic current.

The expressions in Eqs. (10)–(14) are known as the FFCF formulae for the optical conductivity of the single-band systems. It is worth noticing that the present form of the FFCF formulae differs from the common formulae in two important points. First, the selection of diagrams for $\Phi(\mathbf{k},\mathbf{k}_+,\mathbf{k}'_+,\mathbf{k}',i\omega_n,i\omega_{n+})$ and the rearrangement of the summations over wave vectors and frequencies, which lead us to the effective current vertices in Eq. (13), seem to be more precise than the common integration by parts on the time variable of the current-current correlation function,[19] which gives the approximate expression [Eq. (15)] for the effective current vertex. Second, the present treatment of the large-momentum electron-hole excitations by means of the large-momentum Bethe-Salpeter equations is a remedy for the unphysical ω^{-2} singularity of the common FFCF approach when describing the LE excitations.[19]

B. Metallic regime

It is now of relevance to determine the HE part in the optical conductivity [Eq. (14)] in the metallic regime, by using the common approximation for the effective current vertex [Eq. (13)], and compare the result with the expression in Eq. (9).

With the assumption that $\mathcal{G}^0(\mathbf{k}_+, i\omega_{n+}) \approx \mathcal{G}^0[\mathbf{k}, \varepsilon(\mathbf{k}'')/\hbar]$ and $\mathcal{G}^0(\mathbf{k}'', i\omega_{m-}) \approx \mathcal{G}^0[\mathbf{k}'', \varepsilon(\mathbf{k})/\hbar]$, the effective current vertices become

$$j_\alpha(\mathbf{k},\mathbf{k}') \approx \frac{J_\alpha(\mathbf{k}) - J_\alpha(\mathbf{k}')}{\varepsilon(\mathbf{k}') - \varepsilon(\mathbf{k})} \approx \frac{e}{i\hbar\nu_n}[v_\alpha(\mathbf{k}) - v_\alpha(\mathbf{k}')]. \tag{15}$$

For the purpose of brevity, we concentrate once again on the elastic electron scattering on the static disorder. In this case, the force-force correlation function is

$$\mathcal{F}_\lambda(\mathbf{k}' - \mathbf{k}, i\nu_m) = (-)\beta\hbar |V_1(\mathbf{k}' - \mathbf{k})|^2 \delta_{i\nu_m,0}\delta_{\lambda,0}. \tag{16}$$

Inserting Eqs. (15) and (16) into Eqs. (10)–(14), we obtain the HE optical conductivity

$$\Delta\sigma^{\mathrm{HE}}_{\alpha\alpha}(\omega) \approx \frac{i\hbar}{V}\sum_{\mathbf{k}\mathbf{k}'\sigma}\frac{1}{2}j^2_\alpha(\mathbf{k},\mathbf{k}')\frac{f(\mathbf{k}) - f(\mathbf{k}')}{\varepsilon(\mathbf{k}') - \varepsilon(\mathbf{k})}|V_1(\mathbf{k}' - \mathbf{k})|^2 \times \left\{\frac{1}{\hbar\omega + i\eta + \varepsilon(\mathbf{k},\mathbf{k}')} + \frac{1}{\hbar\omega + i\eta + \varepsilon(\mathbf{k}',\mathbf{k})}\right\}, \tag{17}$$

with the wave vectors $\mathbf{k}$ and $\mathbf{k}'$ confined to the extended Brillouin zone (BZ).

In contrast to Eq. (9), the expression in Eq. (17) is characterized by the correct cutoff energy at $\varepsilon_{\max}(\mathbf{k}',\mathbf{k}) = W$. The difference is also in the factor $[f(\mathbf{k}) - f(\mathbf{k}')]/[\varepsilon(\mathbf{k}) - \varepsilon(\mathbf{k}')]$ which appears here instead of the derivative $\partial f(\mathbf{k})/\partial\varepsilon(\mathbf{k})$ in Eq. (9). These results confirm the above statements that all HE intraband single-particle optical excitations in the FFCF approach are related with the real large-momentum electron-hole pairs (of the wave vectors $\mathbf{k}$ and $\mathbf{k}'$), obeying the energy and momentum conservation laws. The conclusion is very general and independent of the detailed structure of the force-force correlation function $\mathcal{F}_\lambda(\mathbf{k}' - \mathbf{k}, i\nu_m)$.

To extend this procedure to the LE region, in particular for the strongly correlated electronic systems with multiple electron scattering channels, one is forced to solve complicated large-momentum Bethe-Salpeter equations. This is not an easy task. However, the answer is simple in the variety of Q1D problems with the electron scattering on the static disorder and/or on the (quasi)static CDW potential. For example, in the metallic regime with $V_1(\mathbf{k}' - \mathbf{k})$ being sufficiently weak, the scattering processes of interest include the states close to the Fermi level. The real part of the electron-hole-pair self-energy is negligible, and there is no essential difference between the expressions in Eq. (9) and (17). In this case, it is possible to recollect the most singular contributions in power of $|V_1(\mathbf{k}' - \mathbf{k})|^2$ to infinity, removing in this way the ω^{-2} singularity characterizing the common FFCF expressions. This result can be obtained by using, for example, the memory-function approach of Appendix A, or the procedure developed in Ref. 24. The resulting optical conductivity is that of the ordinary Drude model, with Γ_α nearly independent of frequency and $m_{\mathrm{eff}} \approx m_{zz}$. As $V_1(\mathbf{k}' - \mathbf{k})$ is increased, Γ_α increases without m_{eff} changing very much.

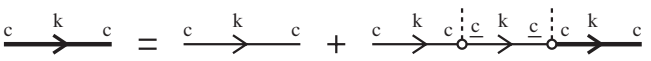

FIG. 3. The Dyson equation for $\mathcal{G}_{cc}(\mathbf{k}, i\omega_n)$ in the pure CDW case in which the commensurability effects are neglected, shown in the two-band representation [Eq. (B1) in Appendix B]. Similar for $\mathcal{G}_{\underline{c}\underline{c}}(\mathbf{k}, i\omega_n)$, $\mathcal{G}_{\underline{c}c}(\mathbf{k}, i\omega_n)$, and $\mathcal{G}_{c\underline{c}}(\mathbf{k}, i\omega_n)$. The dashed lines represent the CDW potential.

V. CLEAN AND DIRTY CDW SYSTEMS

Let us introduce the notation for valence electrons in the ordered-incommensurate CDW systems. Two two-band representations are convenient in this case, the Bloch representation (the band index $L = C$ for the lower completely occupied CDW band and $L = \underline{C}$ for the upper completely empty CDW band) and the representation of the original ($\Delta = 0$) states (the band indices $l = c, \underline{c}$). The wave vector $\mathbf{k}$ is confined to the reduced Brillouin zone of the CDW problem ($|k_z| \le k_F$).

The Dyson equations for electrons, the structure of which is explained in more detail in Appendix B, are illustrated in Fig. 3. The solution is usually given in terms of the Green's functions $\mathcal{G}_{LL}(\mathbf{k}, i\omega_n)$ which are diagonal in the band index L, i.e.,

$$\mathcal{G}_{ll'}(\mathbf{k}, i\omega_n) = \sum_{L=C,\underline{C}} U^*_{\mathbf{k}}(l,L)U_{\mathbf{k}}(l',L)\mathcal{G}_{LL}(\mathbf{k}, i\omega_n),$$

$$\mathcal{G}_{LL}(\mathbf{k}, i\omega_n) = \frac{\hbar}{i\hbar\omega_n - \xi_L(\mathbf{k})}, \tag{18}$$

($l, l' \in \{c, \underline{c}\}$). Here $U_{\mathbf{k}}(l,L)$ are the well-known transformation matrix elements between the electron creation operators in the two representations, Eqs. (B2), $\xi_L(\mathbf{k}) = E_L(\mathbf{k}) - \mu$, and $E_L(\mathbf{k})$ are the dispersions of two CDW bands, Eq. (B4).

A. LE and HE excitations in the ordered clean CDW systems

The application of the FFCF formulae to the ordered clean CDW systems is straightforward, at least for temperatures well below T_{MF}. In this temperature region, the CDW fluctuations are negligible, and the coherent electron scattering on the (static) CDW potential of the magnitude Δ and the wave vector $\mathbf{Q} = (Q_x, Q_z) = (Q_x, 2k_F)$ is only important. The auxiliary HE current-current correlation function is given by

$$\frac{\phi^{\mathrm{HE}}_{\alpha\alpha}(i\nu_n)}{(i\hbar\nu_n)^2} \approx \frac{1}{V}\sum_{\mathbf{k}\sigma}\frac{1}{\beta\hbar^2}\sum_{i\omega_n}\sum_{\lambda\mathbf{k}'i\nu_m}(-)\frac{1}{\beta\hbar}\mathcal{F}_\lambda(\mathbf{k}' - \mathbf{k}, i\nu_m) \times j^2_\alpha(\mathbf{k},\mathbf{k}', i\hbar\omega_m, i\hbar\omega_n)\mathcal{G}(\mathbf{k}, i\omega_n)\mathcal{G}(\mathbf{k}', i\omega_m), \tag{19}$$

with Eq. (16) and $|V_1(\mathbf{k}' - \mathbf{k})|^2 \to \delta_{\mathbf{k}',\mathbf{k}\pm\mathbf{Q}}\Delta^2$, and with the replacements $\mathbf{k} \to c\mathbf{k}$ and $\mathbf{k} \pm \mathbf{Q} \to \underline{c}\mathbf{k}$ to change the (single-band) extended zone representation into the (two band) reduced zone representation. The final result for the optical conductivity[27] is here a direct manifestation of the CDW coherence effects in Eq. (19), which can be easily evaluated and represented by

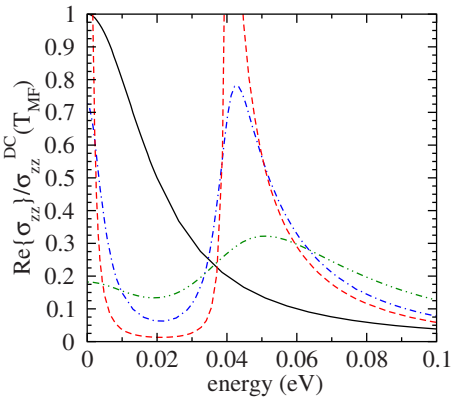

FIG. 4. (Color online) The optical conductivity of the common CDW semiconductors along the highly conducting direction **c** at temperature $T=126$ K, for $2t_{\parallel}=1$ eV, $2t_{\perp}=1$ meV, and $\Delta(126\ \mathrm{K})=20$ meV. $\hbar\Gamma_c^{\mathrm{intra}}=\hbar\Gamma_c^{\mathrm{inter}}=1$, 5 and 20 meV, for the dashed, dot-dashed and dot-dot-dashed line, respectively. The solid line is the optical conductivity at $T>T_{\mathrm{MF}}$ and $\hbar\Gamma_c^{\mathrm{intra}}=20$ meV.

$$j_z^2[\mathbf{k},\mathbf{k}\pm\mathbf{Q},E_{L'}(\mathbf{k}),E_L(\mathbf{k})]|U_{\mathbf{k}}(c,L)|^2|U_{\mathbf{k}}(\underline{c},L')|^2\Delta^2 = |J_z^{LL'}(\mathbf{k})|^2, \tag{20}$$

with the current vertices $J_z^{LL'}(\mathbf{k})$ given by Eq. (B5). The subtraction of the unphysical contributions to the diamagnetic current introduces the gauge-invariance factor $\{i\hbar\nu_n/[E_{\underline{L}}(\mathbf{k}_+)-E_L(\mathbf{k})]\}^2$ in the interband channel. After performing the analytical continuation and replacing the adiabatic term η by the intraband and interband damping energies $\hbar\Gamma_c^{\mathrm{intra}}$ and $\hbar\Gamma_c^{\mathrm{inter}}$, we rederive the gauge-invariant form of the Lee–Rice–Anderson optical conductivity model.[27,28]

The typical results are shown in Fig. 4, for the damping energies $\hbar\Gamma_c^{\mathrm{intra}}=\hbar\Gamma_c^{\mathrm{inter}}=\hbar\Gamma_c$ small compared with 2Δ. In the limit $\hbar\Gamma_c\to 0$, the result is the ideal conductivity of the CDW semiconductors, consisting of the $\omega\approx 0$ intraband contribution of thermally activated charge carriers and the interband term characterized by the square-root singularity at $\hbar\omega=2\Delta$.[21,27] For $T\to 0$, the CDW potential causes the coherent shift of the total optical conductivity spectral weight in the energy region above the threshold energy 2Δ. Being proportional to the interband current vertex $J_z^{C\underline{C}}(\mathbf{k})\propto\sin(\varphi(\mathbf{k})/2)$, Eq. (B5), this type of excitations vanishes already for not too large frequencies.

B. HE excitations in the dirty CDW systems

The HE optical conductivity is now a rather complicated function of energy, in the wide range of energies and temperatures. It is still directly related to the auxiliary current-current correlation function of Eq. (19), but with the product of two modified single-electron Green's functions replaced by the exact electron-hole-pair propagator obtained from the large-momentum Bethe-Salpeter equations. On qualitative grounds, two issues can be meaningfully addressed here. (i) The description of the electron scattering on the (quasi)static CDW potential ($\lambda=0$) in terms of the structure factor $S(\mathbf{q}')$ and comparison of this structure factor with $S(\mathbf{q}')$ estimated by means of other experimental methods. (ii) The precise description of the other ($\lambda\neq 0$), expectedly strong scattering processes, which evidently dominate the HE intraband electron scattering in the whole range of temperatures (both $T<T_{\mathrm{CDW}}$ and $T>T_{\mathrm{CDW}}$). These two types of scattering processes are illustrated in Fig. 5 by the scattering paths $1\to 2$ and $1\to 3\to 4$ (or $1\to 5\to 6$).

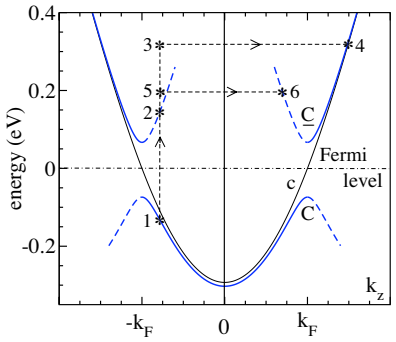

FIG. 5. (Color online) The direct $(1\to 2)$ and the indirect $(1\to 3\to 4$ and $1\to 5\to 6)$ HE optical excitations in the dirty CDW systems, shown in the extended zone representation. The parameters are the same as in Fig. 4. The solid and the dashed lines correspond to the poles in the electron Green's functions associated with the residues $\cos^2[\varphi(\mathbf{k})/2]$ and $\sin^2[\varphi(\mathbf{k})/2]$, respectively [$\varphi(\mathbf{k})$ is defined by Eq. (B3)].

Although the final result for $\sigma_{\alpha\alpha}^{\mathrm{HE}}(\omega)$ is very sensitive to the details in the $\lambda\neq 0$ contributions to the force-force correlation function, the dependence on $\mathcal{F}_0(\mathbf{q}',i\nu_m)=(-)\beta\hbar\delta_{i\nu_m,0}S(\mathbf{q}')$ is generally much simpler. It can be determined by making use of the common parameterization of the structure factor $S(\mathbf{q}')$,[28–30] normalized in the way that $S(\mathbf{q}')=\delta_{\mathbf{q}',\pm\mathbf{Q}}\Delta^2$ at $T=T_{\mathrm{CDW}}$, and represented by the spectral function of the modified single-electron Green's function. Leaving the details of the analysis for Ref. 17, which is devoted to the bad metallic system $BaVS_3$, it may be mentioned here that the result for $\sigma_{\alpha\alpha}^{\mathrm{HE}}(\omega)$ is similar to that of the dirty BCS superconductors,[31] however, with one important difference. While the BCS coherence factors associated with the elastic scattering on the BCS potential are zero for symmetry reasons [namely, the related interband current vertex of Eq. (B5) vanishes], for the CDW case and energies not too large when compared to the threshold energy 2Δ, this scattering channel is equally important as the remaining $\lambda\neq 0$ scattering channels. Moreover, any consistent quantitative examination of the measured spectra at $T<T_{\mathrm{MF}}$, including the estimation of the CDW order parameter Δ, requires the collection of the higher-order terms in the $\lambda\neq 0$ scattering processes, i.e., the systematic treatment of the large-momentum Bethe-Salpeter equations. This makes a general discussion of the dirty CDW systems extremely complicated.

VI. CONCLUSION

The microscopic FFCF theory has been formulated for the HE intraband optical excitations in a wide class of strongly correlated Q1D systems with predominantly incoherent conductivity. It is shown, for example, that the present FFCF theory is able to capture the qualitative aspects of a rather

complicated CDW gap in the optical conductivity of dirty CDW systems. This part of analysis is expected to be of relevance to the detailed quantitative examination of the measured conductivity data in the bad metallic system $BaVS_3$. It is also demonstrated that for perfect and exactly solvable systems with the multicomponent optical conductivity (the ordered CDW case being an example) the FFCF theory gives the same result as the common LE theories, in the whole range of energies. However, the application of the FFCF approach to describe the LE optical excitations in a general strongly correlated case is not a trivial task. Finally, the common LE approaches (which usually result in the generalized Drude formula for the optical conductivity) are found to fail to provide a proper description of the HE optical processes in this case, owing to a strong violation of the energy conservation law.

ACKNOWLEDGMENT

This research was supported by the Croatian Ministry of Science and Technology under Project No. 119-1191458-0512.

APPENDIX A: MEMORY-FUNCTION APPROACH

In order to understand the discrepancy between the longitudinal and the transverse response theories of Secs. III and IV in explaining the LE optical excitations, we use the simplified assumption that $V_1(\mathbf{k}'-\mathbf{k}) \approx V_1(\mathbf{k}'-\mathbf{k}_F)$. This is a good approximation in most Q1D systems. It is even more likely that such situation occurs in the various isotropic two-dimensional or three-dimensional systems. Two integrations in Eq. (17) over $\mathbf{k}$ and $\mathbf{k}'$ are decoupled. Multiplying this expression by $\int d\varepsilon \delta[\varepsilon-\varepsilon(\mathbf{k})]$ and $\int d\varepsilon' \delta[\varepsilon'-\varepsilon(\mathbf{k}')]$, we obtain

$$\Delta\sigma^{\mathrm{HE}}_{\alpha\alpha}(\omega) \approx \frac{i\hbar^2 e^2}{\pi m}\int d\varepsilon \int d\varepsilon' n^{\mathrm{eff}}_{\mathrm{intra},\alpha}(\varepsilon) M''_{\alpha}(\varepsilon') \times \frac{1}{(\varepsilon'-\varepsilon)^2}\frac{f(\varepsilon)-f(\varepsilon')}{\varepsilon'-\varepsilon}\frac{1}{\hbar\omega+i\eta+\varepsilon'-\varepsilon}. \tag{A1}$$

The functions $n^{\mathrm{eff}}_{\mathrm{intra},\alpha}(\varepsilon)$ and $M''_{\alpha}(\varepsilon')$ have the form of the effective density of states

$$n^{\mathrm{eff}}_{\mathrm{intra},\alpha}(\varepsilon) = \frac{m}{V}\sum_{\mathbf{k}\sigma} v^2_{\alpha}(\mathbf{k})\delta[\varepsilon-\varepsilon(\mathbf{k})],$$

$$\hbar M''_{\alpha}(\varepsilon') \approx \sum_{\mathbf{k}'} |V_1(\mathbf{k}'-\mathbf{k}_F)|^2[1-v_{\alpha}(\mathbf{k}')/v_{\alpha}(\mathbf{k}_F)] \times 2\pi\delta[\varepsilon'-\varepsilon(\mathbf{k}')]. \tag{A2}$$

The arguments in these two functions, ε and ε', represent the auxiliary Fermi energies at $T=0$ K measured with respect to μ. $M''_{\alpha}(\varepsilon')$ is the imaginary part of the so-called memory function $M_{\alpha}(\varepsilon')$.[18,26,32]

Using the general arguments of the memory-function theory,[26] which evidently hold for $V_1(\mathbf{k}'-\mathbf{k}) \approx V_1(\mathbf{k}'-\mathbf{k}_F)$ sufficiently weak, we can recollect the contributions in powers of $M_{\alpha}(\omega)/\omega$ to infinity to obtain the memory-function formula for the optical conductivity

$$\sigma_{\alpha\alpha}(\omega) \approx \frac{ie^2 n^{\mathrm{eff}}_{\mathrm{intra},\alpha}}{m\omega}\left\{1-\frac{M_{\alpha}(\omega)}{\omega}+\cdots\right\} = \frac{ie^2 n^{\mathrm{eff}}_{\mathrm{intra},\alpha}}{m}\frac{1}{\omega+M_{\alpha}(\omega)}. \tag{A3}$$

This formula represents the transverse variant of the generalized Drude formula [Eq. (7)].

The memory function $M_{\alpha}(\omega)$ in Eq. (A3) represents the bare HE intraband optical conductivity normalized with respect to the effective number of conduction electrons $n^{\mathrm{eff}}_{\mathrm{intra},\alpha}$,

$$M_{\alpha}(\omega) = \frac{im\omega^2}{e^2 n^{\mathrm{eff}}_{\mathrm{intra},\alpha}}\Delta\sigma^{\mathrm{HE}}_{\alpha\alpha}(\omega), \tag{A4}$$

with $n^{\mathrm{eff}}_{\mathrm{intra},\alpha} = n^{\mathrm{eff}}_{\mathrm{total},\alpha}$ of Eq. (2).

APPENDIX B: CDW AND BCS DYSON EQUATIONS FOR ELECTRONS

In the Q1D models in which the commensurability effects are neglected, the Dyson equations for electrons in the ordered CDW or BCS state can be written as

$$[i\hbar\omega_n - \varepsilon_c(\mathbf{k})]\mathcal{G}_{cc}(\mathbf{k},i\omega_n) + \Delta(\mathbf{k})\mathcal{G}_{\underline{c}c}(\mathbf{k},i\omega_n) = \hbar,$$

$$\Delta^*(\mathbf{k})\mathcal{G}_{cc}(\mathbf{k},i\omega_n) + [i\hbar\omega_n - \varepsilon_{\underline{c}}(\mathbf{k})]\mathcal{G}_{\underline{c}c}(\mathbf{k},i\omega_n) = 0, \tag{B1}$$

using the two-band representation. In the CDW case, the labels $c\mathbf{k}$ and $\underline{c}\mathbf{k}$ refer to the particles of the wave vectors $\mathbf{k}$ and $\mathbf{k}\pm\mathbf{Q}$, respectively. In the BCS case, $c\mathbf{k}$ stands for the particle with $\uparrow\mathbf{k}$, and $\underline{c}\mathbf{k}$ stands for the antiparticle with $\downarrow-\mathbf{k}$ [i.e., $\mathcal{G}_{cc}(\mathbf{k},i\omega_n) \to \mathcal{G}(\mathbf{k},i\omega_n)$ and $\mathcal{G}_{\underline{c}c}(\mathbf{k},i\omega_n) \to -\mathcal{F}^{\dagger}(\mathbf{k},i\omega_n)$ in the common BCS notation].[19]

The solution of Eq. (B1) has the form of Eq. (18). For $\Delta(\mathbf{k})=\Delta$, the residues in the diagonal Green's functions $\mathcal{G}_{ll}(\mathbf{k},i\omega_n)$ are

$$|U_{\mathbf{k}}(c,C)|^2 = |U_{\mathbf{k}}(\underline{c},\underline{C})|^2 = \cos^2\frac{\varphi(\mathbf{k})}{2},$$

$$|U_{\mathbf{k}}(c,\underline{C})|^2 = |U_{\mathbf{k}}(\underline{c},C)|^2 = \sin^2\frac{\varphi(\mathbf{k})}{2}, \tag{B2}$$

with the auxiliary phase $\varphi(\mathbf{k})$ given by

$$\tan\varphi(\mathbf{k}) = \frac{2\Delta}{\varepsilon_{\underline{c}c}(\mathbf{k})} \tag{B3}$$

$[\varepsilon_{\underline{c}c}(\mathbf{k}) = \varepsilon_{\underline{c}}(\mathbf{k}) - \varepsilon_c(\mathbf{k})]$. The related dispersions and the current vertices are

$$E_{\underline{C},C} = \frac{1}{2}[\varepsilon_{\underline{c}}(\mathbf{k}) + \varepsilon_c(\mathbf{k})] \pm \frac{1}{2}\sqrt{\varepsilon^2_{\underline{c}c}(\mathbf{k}) + 4\Delta^2}, \tag{B4}$$

and

$$J_\alpha^{CC}(\mathbf{k}) = \cos^2\frac{\varphi(\mathbf{k})}{2} j_\alpha^{cc}(\mathbf{k}) + \sin^2\frac{\varphi(\mathbf{k})}{2} j_\alpha^{\underline{c}\underline{c}}(\mathbf{k}),$$

$$J_\alpha^{\underline{C}\underline{C}}(\mathbf{k}) = \sin^2\frac{\varphi(\mathbf{k})}{2} j_\alpha^{cc}(\mathbf{k}) + \cos^2\frac{\varphi(\mathbf{k})}{2} j_\alpha^{\underline{c}\underline{c}}(\mathbf{k}),$$

$$J_\alpha^{C\underline{C}}(\mathbf{k}) = [J_\alpha^{\underline{C}C}(\mathbf{k})]^* = \frac{1}{2}\sin\varphi(\mathbf{k})[j_\alpha^{cc}(\mathbf{k}) - j_\alpha^{\underline{c}\underline{c}}(\mathbf{k})]. \quad \text{(B5)}$$

Notice that the bare current vertices are defined by $j_\alpha^{ll}(\mathbf{k}) = (e/\hbar)\partial\varepsilon_l(\mathbf{k})/\partial k_\alpha$. Consequently, for the BCS case, where $\varepsilon_{\underline{c}}(\mathbf{k}) = -\varepsilon_c(-\mathbf{k})$, we obtain $j_\alpha^{\underline{c}\underline{c}}(\mathbf{k}) = j_\alpha^{cc}(\mathbf{k})$, resulting in the disappearance of the current vertex $J_\alpha^{C\underline{C}}(\mathbf{k})$.[19,31]

[1] S. Uchida, T. Ido, H. Takagi, T. Arima, Y. Tokura, and S. Tajima, Phys. Rev. B **43**, 7942 (1991); S. L. Cooper, D. Reznik, A. Kotz, M. A. Karlow, R. Liu, M. V. Klein, W. C. Lee, J. Giapintzakis, D. M. Ginsberg, B. W. Veal, and A. P. Paulikas, *ibid.* **47**, 8233 (1993).

[2] C. S. Jacobsen, D. B. Tanner, and K. Bechgaard, Phys. Rev. B **28**, 7019 (1983); A. Schwartz, M. Dressel, G. Grüner, V. Vescoli, L. Degiorgi, and T. Giamarchi, *ibid.* **58**, 1261 (1998).

[3] L. Degiorgi, B. Alavi, G. Mihály, and G. Grüner, Phys. Rev. B **44**, 7808 (1991).

[4] M. A. Chernikov, L. Degiorgi, E. Felder, S. Paschen, A. D. Bianchi, H. R. Ott, J. L. Sarrao, Z. Fisk, and D. Mandrus, Phys. Rev. B **56**, 1366 (1997).

[5] L. Degiorgi, Rev. Mod. Phys. **71**, 687 (1999) and references therein.

[6] A. J. Millis and P. A. Lee, Phys. Rev. B **35**, 3394 (1987).

[7] J. Ruvalds and A. Virosztek, Phys. Rev. B **43**, 5498 (1991).

[8] M. J. Rozenberg, G. Kotliar, and H. Kajueter, Phys. Rev. B **54**, 8452 (1996).

[9] O. Gunnarsson, M. Calandra, and J. E. Han, Rev. Mod. Phys. **75**, 1085 (2003).

[10] R. A. Gardner, M. Vlasse, and A. Wold, Acta Crystallogr., Sect. B: Struct. Crystallogr. Cryst. Chem. **25**, 781 (1969).

[11] T. Inami, K. Ohwada, H. Kimura, M. Watanabe, Y. Noda, H. Nakamura, T. Yamasaki, M. Shiga, N. Ikeda, and Y. Murakami, Phys. Rev. B **66**, 073108 (2002).

[12] H. Nakamura, H. Imai, and M. Shiga, Phys. Rev. Lett. **79**, 3779 (1997).

[13] G. Mihály, I. Kézsmárki, F. Zámborszky, M. Miljak, K. Penc, P. Fazekas, H. Berger, and L. Forró, Phys. Rev. B **61**, R7831 (2000).

[14] I. Kézsmárki, G. Mihály, R. Gaál, N. Barišić, A. Akrap, H. Berger, L. Forró, C. C. Homes, and L. Mihály, Phys. Rev. Lett. **96**, 186402 (2006).

[15] I. Kézsmárki, Sz. Csonka, H. Berger, L. Forró, P. Fazekas, and G. Mihály, Phys. Rev. B **63** 081106(R) (2001).

[16] S. Fagot, P. Foury-Leylekian, S. Ravy, J.-P. Pouget, and H. Berger, Phys. Rev. Lett. **90**, 196401 (2003).

[17] I. Kupčić and S. Barišić (unpublished).

[18] I. Kupčić, Physica C **391**, 251 (2003); Physica B **344**, 27 (2004).

[19] G. D. Mahan, *Many-particle Physics* (Plenum, New York, 1990).

[20] D. Vollhardt and P. Wölfle, Phys. Rev. B **22**, 4666 (1980).

[21] I. Kupčić, Eur. Phys. J. B **62**, 27 (2008).

[22] D. Pines and P. Noziéres, *The Theory of Quantum Liquids I* (Addison-Wesley, New York, 1989).

[23] J. M. Ziman, *Electrons and Phonons* (Oxford University Press, London, 2004).

[24] I. Kupčić and S. Barišić, Fiz. A **14**, 47 (2005).

[25] I. Kupčić and S. Barišić, Phys. Rev. B **75**, 094508 (2007).

[26] W. Götze and P. Wölfle, Phys. Rev. B **6**, 1226 (1972).

[27] P. A. Lee, T. M. Rice, and P. W. Anderson, Solid State Commun. **14**, 703 (1974).

[28] G. Grüner, *Density Waves in Solids* (Addison-Wesley, New York, 1994).

[29] P. A. Lee, T. M. Rice, and P. W. Anderson, Phys. Rev. Lett. **31**, 462 (1973).

[30] A. Bjeliš and S. Barišić, J. Phys. (France) Lett. **36**, L-169 (1975).

[31] D. C. Mattis and J. Bardeen, Phys. Rev. **111**, 412 (1958).

[32] T. Giamarchi, Phys. Rev. B **44**, 2905 (1991).